Research Paper

Journal of Chemical Research

Journal of Chemical Research
January-February 2021: 147–158

DOI: 10.1177/1747519820932091
journals.sagepub.com/home/chl
SAGE

Theoretical investigations on the HOMO–LUMO gap and global reactivity descriptor studies, natural bond orbital, and nucleus-independent chemical shifts analyses of 3-phenylbenzo[*d*] thiazole-2(3*H*)-imine and its *para*-substituted derivatives: Solvent and substituent effects

Marzieh Miar[1], Abolfazl Shiroudi[2], Khalil Pourshamsian[1], Ahmad Reza Oliaey[1] and Farhad Hatamjafari[1]

Abstract

Natural bond orbital analysis, salvation, and substituent effects of electron-releasing (–CH_3, –OH) and electron-withdrawing (–Cl, –NO_2, –CF_3) groups at *para* positions on the molecular structure of synthesized 3-phenylbenzo[*d*] thiazole-2(3*H*)-imine and its derivatives in selected solvents (acetone, toluene, and ethanol) and in the gas phase by employing the polarizable continuum method model are studied using the M06-2x method and 6-311++G(d,p) basis set. The relative stability of the studied compounds is influenced by the possibility of intramolecular interactions between substituents and the electron donor–acceptor centers of the thiazole ring. Furthermore, atomic charges, electron density, chemical thermodynamics, energetic properties, dipole moments, and nucleus-independent chemical shifts of the studied compounds and their relative stability are considered. The dipole moment values and the highest occupied molecular orbital–lowest unoccupied molecular orbital energy gaps reveal different charge-transfer possibilities within the considered molecules. Finally, natural bond orbital analysis is carried out to picture the charge transfer between the localized bonds and lone pairs.

Keywords

3-phenylbenzo[*d*]thiazole-2(3*H*)-imines, density functional theory, nucleus-independent chemical shift, natural bond orbital, polarizable continuum model, solvent effects

Date received: 16 April 2020; accepted: 15 May 2020

Introduction

Heterocycles are the largest and one of the classical divisions of organic chemistry. They are of immense importance not only biologically but also industrially. The majority of pharmaceutical products that mimic natural products with biological activity are heterocycles. Fused heterocyclic compounds are key valuable and structural scaffolds in a broad variety of natural products, drug molecules, and functional materials.[1–3] Among them, research on benzothiazoles, organosulfur heterocyclic compounds has become a rapidly developing and increasingly active topic. Such compounds are used as building blocks in organic synthesis due to their wide range of biological activities, and they form core in various drugs such as anticancer, antimicrobial, anti-asthmatic, antitumor, antibacterial, antitubercular, anti-convulsant, anti-HIV, anti-inflammatory, antifungal, antiproliferative, antiviral, anti-Alzheimer, antimalarial, and anti-diabetic, agents.[4–13]

[1]Department of Chemistry, Islamic Azad University, Tonekabon, Iran
[2]Young Researchers and Elite Club, Islamic Azad University, Tehran, Iran

Corresponding authors:
Abolfazl Shiroudi, Young Researchers and Elite Club, Islamic Azad University, East Tehran Branch, Tehran 18661-13118, Iran.
Email: abolfazl.shiroudi@iauet.ac.ir

Khalil Pourshamsian, Department of Chemistry, Islamic Azad University, Tonekabon Branch, Tonekabon 46841-61167, Iran.
Email: kshams49@gmail.com

Herein, we report a facile, environmentally friendly method for intramolecular cyclization under solvent-free conditions. The reaction occurs in two steps in the presence of sodium *tert*- butoxide as a strong base. Finally, the challenges of using organic solvents in industrial processes are discussed from the perspective of cost, stability, and safety. We suggest that a holistic view of solvent effects, the mechanistic elucidation of these effects, and careful consideration of the challenges associated with solvent use could assist researchers in choosing and designing improved solvent systems for targeted benzothiazole biomass conversion processes.[14–16]

At present, density functional theory (DFT) is accepted as a popular post-Hartree–Fock (HF) approach for the ab initio computation of molecular structures, and the energies of molecules.[17] It has proved to be extremely useful in the study of the electronic structures of molecules. There are several basic approaches available for modeling molecular systems in solution. One of them is the implicit treatment of solvent molecules,[18] Self-consistent reaction field (SCRF) models employ this approach,[19] with the polarizable continuum model (PCM) being the first proposed SCRF method. Employing the PCM model in DFT is a good method while investigating solvent effects.[20] In this study, we present an overview of organic solvent effects. In our pursuit of an improved synthetic method for the preparation of organic compounds, the M06-2x quantum method[21] utilizing the 6-311++G(d,p) basis set[22] has been used in the studied solvents (toluene, acetone, and ethanol), and the obtained data has been compared with the same properties in the gas phase in order to determine their electronic and spectroscopic properties and to benefit from two major types of effects: solvent effects on solubility of benzothiazole components and solvent effects on chemical thermodynamics including those affecting the products.[23,24] Moreover, an attempt is made to supply further qualitative chemical insights using the donor-acceptor interaction energies, nucleus-independent chemical shift (NICS) techniques,[25–29] and natural bond orbital (NBO) analysis.[30,31] This study aims to present quantitative answers to the following questions[32] concerning the solvent and substituent effects on the electronic structures of 3-substituted 3-phenylbenzo[*d*]thiazole-2(3*H*)-imines:

1. How do the donor-acceptor interactions influence the occupancies of the involved bonds?
2. Is there a relationship between the highest occupied molecular orbital (HOMO)-lowest unoccupied molecular orbital (LUMO) gaps in the considered compounds?
3. How does the resonance energy relate to the donor-acceptor interactions in the considered compounds?

As a final point, we justify the obtained results with global reactivity descriptor studies in order to give a deeper insight into the solvent and substituent effects.

Theory and computational details

All quantum chemical calculations were performed using the Gaussian 09 program.[33] The molecular structures were visualized based on the output data of the DFT calculations using the GaussView program.[34] Geometry optimizations and frequency calculations were carried out using DFT along with the M06-2x exchange-correlation functional in conjunction with the split-valence 6-311++G(d,p) basis function because of its high accuracy in achieving geometries, zero-point energy (ZPE)[35] and frequencies[36] combined with computational efficiency.[37,38]

All the optimized structures gave no negative vibrational modes showing that all structures were stationary points in the geometry optimization procedures. The rationale for choosing the M06-2x functional was based on the fact that it is the best for studies involving main group thermochemistry, kinetics, noncovalent interactions, and electronic excitation energies to the valence and Rydberg states. The M06-2x functional and its analogs are dedicated to precise energetic considerations.[39]

The nature of all the optimized structures are determined based on the harmonic vibrational frequency calculations determined at the same level of theory to confirm that a minimum on the potential energy surface was achieved under the imposed constraint of the indicated symmetry.[40]

The NBO populations, atomic charges, frontier molecular orbital (FMO) properties, second-order perturbation stabilization energies, and dipole moments are considered at the same theoretical level using the NBO 5.0 program.[41] Furthermore, the aromaticity index NICS values for all the studied compounds are estimated within the gauge-included atomic orbital (GIAO) method at the M06-2x/6-311++G(d,p) level of theory. Finally, in order to estimate the effect of the liquid environment, the geometries of the studied compounds are re-optimized at the same level of theory in three different solvents: non-polar toluene ($\varepsilon = 2.374$), polar aprotic acetone ($\varepsilon = 20.493$), and polar protic ethanol ($\varepsilon = 24.852$).

Results and discussion

The synthesis of 3-phenylbenzo[*d*]thiazole-2(3*H*)-imine and its *para*-substituted derivatives (**3a–f**) was carried out by reaction of different synthesized *N*-acyl-*N*′-aryl thioureas (**1a–f**) with diazonium salts (**2**). The optimized structures of all the compounds (see Scheme 1) were then investigated by comprehensive computational studies and are presented in Supplemental Figure S1.

Energy and thermodynamic parameters

The structures and numbering of the three-substituted 3-phenylbenzo[*d*]thiazole-2(3*H*)-imines are shown in Scheme 2. The computed corrected total energy (E_{corr}) and Gibbs free energies (G), relative energies (ΔE) as well as the relative Gibbs free energies (ΔG) using the M06-2x method in different solvents and gas phases at $T = 298$ K are listed in Table 1.

The relative energies and Gibbs free energies in acetone are more stable by about 0.46–18.31 and 0.63–18.77 kcal/mol, respectively, than those determined in the solvents. The major difference between the obtained energies and Gibbs free energies were found in the gas phase (18.31 and 18.77 kcal/mol, respectively, for the OH substituent). The

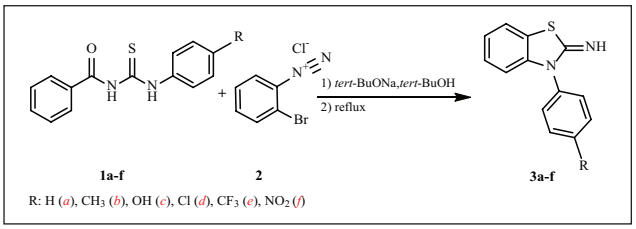

Scheme 1. The synthetic route of 3-phenylbenzo[*d*]thiazole-2(3*H*)-imine and its derivatives.

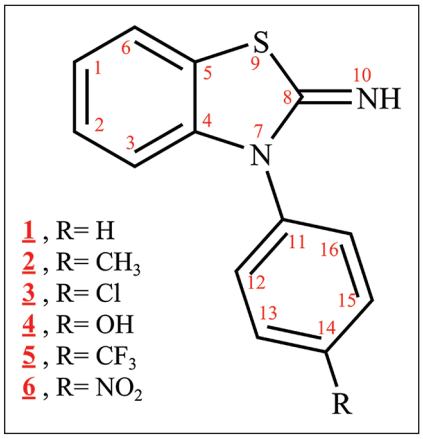

Scheme 2. The synthesis of the studied compounds.

order of stability in the considered solvent and gas phases is $Cl > CF_3 > NO_2 > OH > CH_3 > H$. The obtained results show that the stability increases with increasing electron-withdrawing substituents.

On other hand, all the species were stabilized more or less by the solvent dielectric constant, where the corrected total energy (E_{corr}) decrease in polar solvents (ethanol and acetone) was more than in the non-polar solvent (toluene). The solute-solvent interactions further stabilized the structures compared to either the non-polar solvent (toluene) or in the gas phase. It is noted that the values of solvation energies (E_{solv}) are higher in the case of ethanol and acetone compared to toluene, which agrees with the polar character of the considered compounds (Table 1). The polar solvents (ethanol and acetone) stabilized the studied compounds through hydrogen bonding and dipole-dipole interactions more than the non-polar solvent (toluene).

Dipole moments

The dipole moment (μ) prediction is an important issue which is associated with the molecular stability in polar environments.[42] In this work, the experimental dipole moment is not known. The calculated dipole moments in different environments (i.e. toluene, acetone, and ethanol) are shown in Table 2. The influence of the polar environment (i.e. acetone and ethanol) is notable in comparison to the dipole moment values in both phases. The order of the calculated dipole moment values are $NO_2 > CF_3 > Cl > CH_3 > H > OH$. Among the considered compounds **1**–**6**, compound **6** ($X = NO_2$ substituent) has the highest dipole moment in the studied solvents and gas phases because it has a higher dipole interaction. The order of the calculated dipole moment values for the studied molecules in solvents with different polarity (ethanol > acetone > toluene) the arising results related to the increase of the dielectric constant which corresponds to the dielectric constant value orders that it will be increased with increasing dielectric constant (Table 2).

The highest dipole moment for all the compounds was observed in ethanol. As can be seen in Table 2, the dipole moment increases from the gas phase to a more polar solvent, with the highest dipole moment occurring for compound **6** with a NO_2 substituent in ethanol solution with a value of ~5.94, while compound **1** has the lowest dipole moment in the gas phase (~1.91). It is noticeable that dipole moments are related to the influence of the nature of the substituents at the N7 position. In this work, higher dipole moment values were observed in the compounds possessing in electron acceptors (i.e. NO_2, Cl, CF_3) compared to those with electron-donor groups (i.e. H, CH_3, OH) in the studied solvents and gas phase. This is explained by consideration of the charge values on the atoms of the THREE-substituted six-membered ring. It is well known that in the studied compounds, the nitrogen N7 atom carries the most negative charge (Table 3).

Solvent effects

Solvent effects are significant in stability phenomena because polarity differences between tautomers can induce important changes in their relative energies in solution.[43] PCM calculations were used to evaluate the solvent effects on the 3-phenylbenzo[*d*]thiazole-2(3*H*)-imine and its *para*-substituted derivatives. It is noted that the PCM model does not consider the presence of explicit solvent molecules; therefore, specific solute-solvent interactions are not defined and the studied solvation effects arise only from mutual solute-solvent electrostatic polarization.[43] The lowest energy values of compounds **1**–**6** are obtained from aqueous solution calculations. The dipole moments are increased by increasing the solvent polarity and changing from gas to solution phases. Hence, increased stability with an electron-donating group in polar solvents could be associated with an increase of dipole moments (Table 2). Plots of the dipole moment of the considered compounds *versus* dielectric constants are shown in Figure 1.

The charge distributions of dipolar compounds are often altered considerably in the presence of the solvent field.[44] We have studied the charge distribution for compounds **1**–**6** in solvents and in the gas phase using the NBO technique. The charge distribution with increasing polarity varies differently for any atoms in solvents, for example, a regular increase of the negative charge was found for the N7 atom derivatives when passing from the gas phase to a more polar solvent (Table 2). The charge distribution on the N7 atom is affected by the nature of the substituent and the polarity of the solvents.

Table 1. Total energies and Gibbs free energies (in Hartree), relative energies and Gibbs free energy, ΔG (in kcal/mol) and solvation energies (ΔE_{Solv}) for three-substituted 3-phenylbenzo[*d*] thiazole-2(3*H*)-imines **1**–**6** (P = 1 atm, T = 298 K).

Substituent	Parameter	Gas (ε = 1.0)	Toluene (ε = 2.374)	Acetone (ε = 20.493)	Ethanol (ε = 24.852)
–H (1)	E_{corr}	−1008.800	−1008.819	−1008.825	−1008.822
	G_{corr}	−1008.840	−1008.859	−1008.866	−1008.863
	ΔE_{corr}	15.662	3.666	0.000	1.837
	ΔG_{corr}	15.949	4.084	0.000	1.731
	ΔE_{Solv}	0.000	−11.996	−15.662	−13.825
–Me (2)	E_{corr}	−1048.080	−1048.100	−1048.105	−1048.102
	G_{corr}	−1048.121	−1048.142	−1048.148	−1048.145
	ΔE_{corr}	16.241	3.731	0.000	1.856
	ΔG_{corr}	16.692	3.797	0.000	1.884
	ΔE_{Solv}	0.000	−12.510	−16.241	−14.384
–Cl (3)	E_{corr}	−1468.410	−1468.431	−1468.436	−1468.433
	G_{corr}	−1468.452	−1468.473	−1468.478	−1468.476
	ΔE_{corr}	15.959	3.272	0.000	1.775
	ΔG_{corr}	16.433	3.343	0.000	1.616
	ΔE_{Solv}	0.000	−12.686	−15.959	−14.184
–OH (4)	E_{corr}	−1084.021	−1084.042	−1084.050	−1084.049
	G_{corr}	−1084.062	−1084.084	−1084.092	−1084.091
	ΔE_{corr}	18.306	5.077	0.000	0.462
	ΔG_{corr}	18.766	5.041	0.000	0.626
	ΔE_{Solv}	0.000	−13.229	−18.306	−17.844
–CF_3 (5)	E_{corr}	−1345.847	−1345.866	−1345.872	−1345.869
	G_{corr}	−1345.893	−1345.912	−1345.918	−1345.915
	ΔE_{corr}	15.447	3.792	0.000	1.674
	ΔG_{corr}	15.632	3.881	0.000	1.728
	ΔE_{Solv}	0.000	−11.655	−15.447	−13.774
–NO_2 (6)	E_{corr}	−1213.287	−1213.308	−1213.314	−1213.310
	G_{corr}	−1213.330	−1213.352	−1213.358	−1213.353
	ΔE_{corr}	17.342	3.912	0.000	2.874
	ΔG_{corr}	17.449	3.902	0.000	2.920
	ΔE_{Solv}	0.000	−13.430	−17.342	−14.468

ΔE_{solv} = (E_{corr} in solvent − E_{corr} in gas).

Table 2. Calculated dipole moment of the optimized compounds **1**–**6** (in Debyes) in the studied solvent and gas phases.

Substituent	Gas (ε = 1.00)	Toluene (ε = 2.374)	Acetone (ε = 20.493)	Ethanol (ε = 24.852)
X = H [**1**]	1.9064	1.9685	2.0949	2.1042
X = Cl [**2**]	2.6144	2.6481	2.6672	2.6940
X = CH_3 [**3**]	2.0122	2.1487	2.2518	2.2748
X = OH [**4**]	1.7086	2.0246	2.3897	2.4145
X = CF_3 [**5**]	3.7871	3.8093	3.8620	3.8774
X = NO_2 [**6**]	5.7918	5.8150	5.8889	5.9361

Table 3. The calculated natural atomic charges of compounds **1**–**6**.

Atom	H (**1**)	CH_3 (**2**)	Cl (**3**)	OH (**4**)	CF_3 (**5**)	NO_2 (**6**)
C4	0.17376	0.17432	0.17195	0.17411	0.16989	0.16800
C5	−0.20438	−0.20499	−0.20450	−0.20493	−0.20340	−0.20311
N7	−0.51340	−0.51206	−0.51398	−0.51070	−0.51524	−0.51537
C8	0.33961	0.34003	0.33817	0.33997	0.33725	0.33565
S9	0.30698	0.30570	0.31156	0.30587	0.31535	0.32064
N10	−0.72158	−0.72200	−0.72168	−0.72398	−0.72088	−0.71983
C11	0.15776	0.14786	0.15530	0.12327	0.17962	0.19328
H	0.35294	0.35237	0.35456	0.35246	0.35600	0.35771

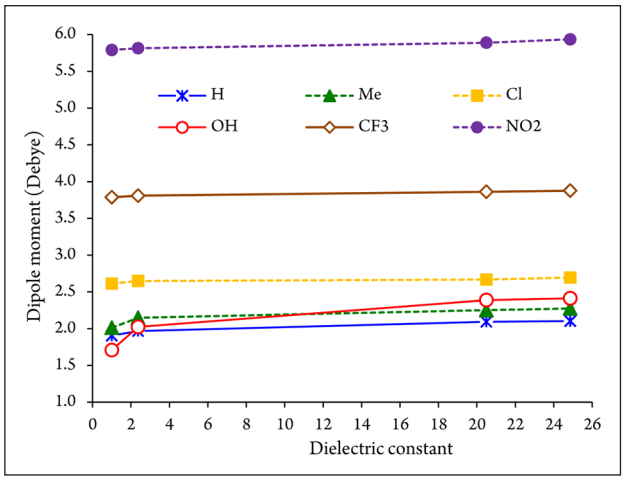

Figure 1. Dielectric constant dependence of the dipole moments for the considered compounds.

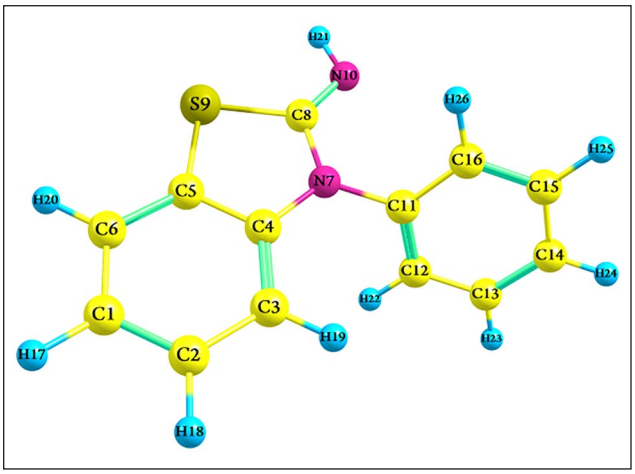

Figure 2. Optimized structure of 3-phenylbenzo[*d*]thiazole-2(3*H*)-imine (compound **1**).

Mulliken atomic charges

The Mulliken[45,46] population analysis is probably the best known of all models for predicting individual atomic charges which is computationally very popular due to its simplicity. Mulliken charges were shown to be highly basis set dependent and unpredictable with marked fluctuations in partial charges.[47] We have studied the charge distribution using NBO techniques in different media. The Mulliken population analysis in compounds **1**–**6** calculated using the NBO method at the M06-2x/6-311++G(d,p) level of theory, and the obtained results are illustrated in detail in Table S1 of the Supplemental material. In the case of benzene rings, all the carbon atoms are expected to be negative, but carbon atoms C4 and C11 are found to be positively charged, which may be due to the attachment of the nitrogen atom N7 in the five-membered ring at these carbon atoms. All the hydrogen atoms in the studied molecules are found to be equally slightly positive as expected, as with other hydrogen atoms in the considered molecules.

As can be seen in Figure 2, the nitrogen atom (N10) has more negative charges whereas all the hydrogen atoms have positive charges (see Table S1 in the Supplemental material). The result suggests that the atoms bonded to nitrogen atoms (H21 and C11) are electron acceptors and also indicates the charge transfer from them (H21 and C11) to the nitrogen atom (N10). The relationship between the C–H wavenumber shifts and calculated Mulliken charges of C16 (−0.1833e) and N10 (−0.7216e) also indicates that they take part in intramolecular hydrogen bonding. The influence of electronic effect resulting from the hyperconjugation and induction of the substituent group (X: H, Me, Cl, OH, CF_3, NO_2) in the aromatic six-membered ring causes a large negatively charged value on the carbon atom C14.

These calculations showed the electronegative nature of the O, S, and N atoms. In compound **6**, the hydrogen atom H21 was the most electropositive atom among all the hydrogen atoms (see Figure 2). The proton of the triazole NH group possesses the highest value of 0.35771e. In compounds **1**–**6**, the charges at this H-site (H21 atom) were calculated to be 0.35294e, 0.35237e, 0.35456e, 0.35246e, 0.35600e, and 0.35771e, respectively. The order of the charge density at the NH hydrogen of the triazole ring is **6** > **5** > **3** > **1** > **4** > **2**. This order agrees with the chemical sense where the electron-releasing substituent, namely the CH_3 group (compound **2**), decreases the positive charge at this H-site, while the NO_2 substituted derivative (compound **6**) has the highest positive NH proton, which agrees with its high electron-withdrawing character (−0.71983e), although the substituent is not directly attached to the triazole ring. It should be pointed out that the nitrogen atom corresponding to the NH group in the studied compounds has high negative values. The charge on this nitrogen atom (N10) is in the range of −0.71983e to −0.72398e for the considered compounds. Instead, the charge on the nitrogen atom of the ring (N3) of compounds **1**–**6** is calculated to be less (−0.51340e, −0.51206e, −0.51398e, −0.51070e, −0.51524e, and −0.51537e, respectively) negative than that on the NH one (N6 atom). Compound **6** showed a high positive value for the hydrogen atom (H21) associated with the NO_2 group, 0.35771e, resulting from its bonding to the six-membered ring which is connected to the triazole ring (see Table S1 in the Supplemental material).

Furthermore, carbon atoms C4, C8, and C11 are negatively charged except for those attached to the strong electronegative N atom (see Table S1 in the Supplemental material). The charge on the carbon atom in the six-membered ring of compounds **1**–**6** are calculated as −0.19844e (X=H), −0.02914e (X=CH_3), −0.04327e (X=Cl), 0.32693e (X=OH), −0.14892e (X=CF_3), and 0.06419e (X=NO_2), respectively. The carbon atom of the C–Cl bond in compound **3** has a less negative charge of −0.04327e than that of the C–CF_3 bond of compound **5** (−0.14892e) that is in agreement with the higher electronegative nature of the chlorine atom (0.01100e) compared to the carbon atom in the CF_3 group (1.08796e). The phenolic oxygen atom of compound **4** has the highest negative value of −0.68134e. As a result, the attached carbon atom, C14 (0.32693e) in compound **4** is found to have the most positive aromatic carbon atom (see Table S1 in the Supplemental material).

FMO analysis

Molecular orbitals and their properties such as energy are useful for physicists and chemists. This is also used in frontier electron density for predicting the most reactive position in π-electron systems and also explains several types of reactions in conjugated systems.[48] FMO analysis is widely employed to explain the optical and electronic properties of organic compounds.[49] Knowledge of the HOMO and LUMO, and their properties namely their energy, is very useful to gauge the chemical reactivity of molecules. During molecular interactions, the LUMO accepts electrons and its energy corresponds to the electron affinity (EA), while the HOMO represents electron donors and its energy is associated with the ionization potential (IP).[48]

The HOMO-LUMO energy gap explains the concluding charge transfer interaction within the molecule and is useful in determining molecular electrical transport properties. A molecule with a high frontier orbital gap (HOMO-LUMO energy gap) has low chemical reactivity and high kinetic stability,[50–52] because it is energetically unfavorable to add an electron to the high-lying LUMO in order to remove electrons from the low-lying HOMO. For instance, compounds that have a high HOMO-LUMO energy gap are stable, and hence are chemically harder than compounds having a small HOMO-LUMO energy gap.[52] Thus, it is clear from Table 4 that compound **1** (X=H) is hard and more stable (less reactive), while compound **6** (X=NO_2) is soft and the least stable of all (more reactive) in the studied solvents and gas phases. The HOMO-LUMO energy gap decreases from compounds **1** to **6**. The minimum energy gap is achieved with a NO_2 substituent in the considered solvent and gas phases. Thus, this substituent increases the reactivity of the five-membered ring. The computed HOMO and LUMO energies are listed in Table 5 in all the media considered.

The global electrophilicity index (ω), introduced by Parr et al.,[53,54] is based on thermodynamic properties and measures the favorable change in energy when a chemical system attains saturation by the addition of electrons. It can be defined as the decrease in energy due to the flow of electrons from the donor (HOMO) to the acceptor (LUMO) in molecules. It also plays an important role in determining the chemical reactivity of a system and is defined as follows

$$\omega = \frac{\mu^2}{2\eta} \tag{1}$$

where η denotes the global chemical hardness and μ represents the electronic chemical potential which describes the charge transfer within a system in the ground state as follows[55]

$$\eta = \frac{E_{\mathrm{LUMO}} - E_{\mathrm{HOMO}}}{2} \tag{2}$$

$$\mu = \frac{E_{\mathrm{HOMO}} + E_{\mathrm{LUMO}}}{2} \tag{3}$$

Compounds having greater values of chemical potential are more reactive than those with small electronic chemical potentials. It is clear that compound **6** is the most reactive while compound **1** is the least reactive of all. Similarly, the electronegativity (χ) is a measure of the attraction of an atom for electrons in a covalent bond; thus, compound **6** has higher electronegativity (χ), and it does exhibit high charge flow. Also, the obtained results show that compound **6** (X=NO_2) is strongly electrophilic, while compound **2** (X=CH_3) is nucleophilic (see Table 4).

Moreover, $\Delta N_{\max}$ represents the maximum electronic charge, S is the global softness, and χ denotes the absolute electronegativity, which is used to calculate the electron transfer direction and is given by

$$\Delta N_{\max} = -\frac{\mu}{\eta} \tag{4}$$

$$\chi = -\mu \tag{5}$$

$$S = \frac{1}{\eta} \tag{6}$$

The absolute electronegativity is a good measure of the molecular ability to attract electrons to itself [χ=(IP + EA)/2] where EA and IP are the electron affinity and IP, respectively. It is noted that a small IP value along with a high EA is equal to high nucleophilicity and high electrophilicity, respectively. As can be seen from Table 4, the *para* functional group will further influence the HOMO and LUMO energy levels in the studied compounds (**1**–**6**). Electron-donating groups lead to an increase in the energy levels of the frontier orbitals whereas electron-withdrawing groups have the opposite effect. The energy levels increase in order from the most strongly electron-withdrawing group (–NO_2) to the most strongly electron-donating group (–CH_3). The CH_3 substituent (compound **2**) has the lowest IP and therefore is the most nucleophilic species. All the considered compounds in the solvents and gas phases have positive $\Delta N_{\max}$ values and act as electron acceptors from their environment. The global reactivity of compounds **1**–**6** is discussed in terms of the HOMO and LUMO energies, the energy gap $E_{\mathrm{LUMO\text{-}HOMO}}$, besides the chemical reactivity descriptors which are computed at the M06-2x/6-311++G(d,p) level, and are presented in Table 4.

The values of the LUMO-HOMO energy gap reflect the chemical activity of the molecule. The decrease in the HOMO-LUMO energy gap explains the eventual charge transfer interaction taking place within the studied compounds [**1**–**6**] because of the strong electron-accepting ability of the electron acceptor group (Table 4). As a result, the stability of the studied compounds is **1** > **3** > **2** > **4** > **5** > **6**. The calculated results show that compounds **1** and **6** have the highest and lowest stabilities, respectively, in the solvent and gas phases. Similarly, the calculated $\Delta N_{\max}$ values revealed the same trend (see Table 4). Moreover, because of the larger HOMO-LUMO energy gap, the global hardness increases for compounds **1**–**6** as follows: **1** > **3** > **2** > **4** > **5** > **6**, and the chemical reactivity decreases in the opposite order: **1** < **3** < **2** < **4** < **5** < **6**.

Table 4. Global reactivity descriptors calculated for 3-phenylbenzo[*d*]thiazole-2(3*H*)-imine and its *para*-substituted derivatives (**1**–**6**) at the M06-2x/6-311++G(d,p) level of theory.

Substituent	Paramater										
	HOMO (a.u.)	LUMO (a.u.)	ΔE (eV)	μ (eV)	η (eV)	ω (eV)	S (eV)	χ (eV)	ΔN_{max} (eV)	IP (eV)	EA (eV)
Gas (ε = 1.00)											
H	−0.25760	−0.00555	6.859	−3.580	3.429	50.858	7.935	3.580	28.410	7.010	0.151
CH_3	−0.25536	−0.00560	6.796	−3.551	3.398	50.474	8.008	3.551	28.432	6.949	0.152
Cl	−0.26253	−0.01111	6.841	−3.723	3.421	55.131	7.955	3.723	29.616	7.144	0.302
OH	−0.25555	−0.00798	6.737	−3.586	3.368	51.928	8.079	3.586	28.966	6.954	0.217
CF_3	−0.26749	−0.02327	6.646	−3.956	3.323	64.081	9.634	3.956	32.397	7.279	0.633
NO_2	−0.27284	−0.06525	5.649	−4.600	2.824	101.929	8.189	4.600	44.318	7.424	1.776
Toluene (ε = 2.374)											
H	−0.25765	−0.0056	6.859	−3.582	3.429	50.897	7.935	3.582	28.420	7.011	0.152
CH_3	−0.25589	−0.00563	6.810	−3.558	3.405	50.589	7.992	3.558	28.436	6.963	0.153
Cl	−0.26263	−0.01125	6.840	−3.726	3.420	55.237	7.956	3.726	29.647	7.147	0.306
OH	−0.25657	−0.00877	6.743	−3.610	3.371	52.595	8.071	3.610	29.137	6.982	0.239
CF_3	−0.26742	−0.02410	6.621	−3.966	3.311	64.654	9.691	3.966	32.602	7.277	0.656
NO_2	−0.27273	−0.06636	5.616	−4.614	2.808	103.139	8.220	4.614	44.711	7.421	1.806
Acetone (ε = 20.493)											
H	−0.25774	−0.00547	6.865	−3.581	3.432	50.837	7.928	3.581	28.391	7.013	0.149
CH_3	−0.25592	−0.00584	6.805	−3.561	3.403	50.719	7.997	3.561	28.482	6.964	0.159
Cl	−0.26277	−0.01115	6.847	−3.727	3.423	55.200	7.948	3.727	29.623	7.150	0.303
OH	−0.25719	−0.00972	6.734	−3.631	3.367	53.290	8.082	3.631	29.349	6.998	0.264
CF_3	−0.26712	−0.02487	6.592	−3.973	3.296	65.150	9.755	3.973	32.798	7.269	0.677
NO_2	−0.27243	−0.06741	5.579	−4.624	2.789	104.278	8.256	4.624	45.105	7.413	1.834
Ethanol (ε = 24.852)											
H	−0.25774	−0.00549	6.864	−3.581	3.432	50.849	7.929	3.581	28.396	7.013	0.149
CH_3	−0.25591	−0.00583	6.805	−3.561	3.403	50.711	7.997	3.561	28.480	6.964	0.159
Cl	−0.26274	−0.01131	6.842	−3.729	3.421	55.294	7.955	3.729	29.659	7.150	0.308
OH	−0.25719	−0.00961	6.737	−3.630	3.368	53.223	8.078	3.630	29.324	6.998	0.262
CF_3	−0.26716	−0.02488	6.593	−3.973	3.296	65.164	9.783	3.973	32.800	7.270	0.677
NO_2	−0.27254	−0.06810	5.563	−4.635	2.782	105.067	8.255	4.635	45.340	7.416	1.853

HOMO: highest occupied molecular orbital; LUMO: unoccupied molecular orbital; IP: ionization potential; EA: electron affinity.

Table 5. The second-order perturbation energies E_2 (in kcal/mol) for the most important charge transfer interactions in compounds **1**–**6** in the gas phase.

Donor NBO (*i*)	ED(*i*) (a.u.)	Acceptor NBO(*j*)	ED(*j*) (a.u.)	Interaction type	E_2 (kcal/mol)					
					X = H	X = CH_3	X = Cl	X = OH	X = CF_3	X = NO_2
$\sigma_{N7–C8}$	1.97864	$\sigma^*_{C3–C4}$	0.02373	$\sigma_{N7–C8} \rightarrow \sigma^*_{C3–C4}$	3.12	3.13	3.11	3.13	3.08	3.07
		$\sigma^*_{C4–N7}$	0.03489	$\sigma_{N7–C8} \rightarrow \sigma^*_{C4–N7}$	2.62	2.61	2.61	2.61	2.60	2.57
		$\sigma^*_{N7–C11}$	0.04266	$\sigma_{N7–C8} \rightarrow \sigma^*_{N7–C11}$	2.52	2.52	2.52	2.53	2.51	2.50
		$\sigma^*_{C8–N10}$	0.00937	$\sigma_{N7–C8} \rightarrow \sigma^*_{C8–N10}$	1.65	1.66	1.62	1.65	1.60	1.56
		$\sigma^*_{N10–H21}$	0.00794	$\sigma_{N7–C8} \rightarrow \sigma^*_{N10–H21}$	2.64	2.64	2.66	2.63	2.67	2.69
		$\sigma^*_{C11–C12}$	0.02670	$\sigma_{N7–C8} \rightarrow \sigma^*_{C11–C12}$	1.03	1.01	1.04	0.96	1.11	1.19
		$\pi^*_{C11–C12}$	0.36802	$\sigma_{N7–C8} \rightarrow \pi^*_{C11–C12}$	0.89	0.90	0.93	0.98	0.92	0.93
$\sigma_{C8–N10}$	1.99183	$\sigma^*_{N7–C8}$	0.07155	$\sigma_{C8–N10} \rightarrow \sigma^*_{N7–C8}$	1.62	1.64	1.59	1.64	1.55	1.50
		$\sigma^*_{N10–H21}$	0.00794	$\sigma_{C8–N10} \rightarrow \sigma^*_{N10–H21}$	0.71	0.71	0.72	0.71	0.72	0.72
$\pi_{C8–N10}$	1.98974	$\pi^*_{C8–N10}$	0.30326	$\pi_{C8–N10} \rightarrow \pi^*_{C8–N10}$	1.77	1.77	1.76	1.78	1.74	1.71
$\sigma_{C4–C5}$	1.96633	$\sigma^*_{C3–C4}$	0.02373	$\sigma_{C4–C5} \rightarrow \sigma^*_{C3–C4}$	5.64	5.61	5.68	5.62	5.73	5.76
		$\sigma^*_{C3–H19}$	0.01307	$\sigma_{C4–C5} \rightarrow \sigma^*_{C3–H19}$	2.24	2.24	2.24	2.24	2.25	2.27
		$\sigma^*_{C4–N7}$	0.03489	$\sigma_{C4–C5} \rightarrow \sigma^*_{C4–N7}$	1.56	1.55	1.54	1.55	1.54	1.52
		$\sigma^*_{C5–C6}$	0.02103	$\sigma_{C4–C5} \rightarrow \sigma^*_{C5–C6}$	4.83	4.84	4.83	4.84	4.83	4.84
		$\sigma^*_{C6–H20}$	0.01400	$\sigma_{C4–C5} \rightarrow \sigma^*_{C6–H20}$	2.55	2.55	2.54	2.56	2.52	2.49
		$\sigma^*_{N7–C11}$	0.04266	$\sigma_{C4–C5} \rightarrow \sigma^*_{N7–C11}$	4.60	4.60	4.62	4.58	4.62	4.64
		$\sigma^*_{C8–S9}$	0.08416	$\sigma_{C4–C5} \rightarrow \sigma^*_{C8–S9}$	0.71	0.71	0.71	0.71	0.70	0.70

(Continued)

Table 5. (Continued)

Donor NBO (*i*)	ED(*i*) (a.u.)	Acceptor NBO(*j*)	ED(*j*) (a.u.)	Interaction type	E_2 (kcal/mol)					
					X = H	X = CH_3	X = Cl	X = OH	X = CF_3	X = NO_2
π_{C4-C5}	1.64246	π^*_{C1-C6}	0.35810	$\pi_{C4-C5} \rightarrow \pi^*_{C1-C6}$	30.29	30.39	–	30.41	–	–
		π^*_{C2-C3}	0.35677	$\pi_{C4-C5} \rightarrow \pi^*_{C2-C3}$	24.20	24.20	–	24.18	–	–
$LP(1)_{N7}$	1.67385	π^*_{C2-C3}	0.01442	$LP(1)_{N7} \rightarrow \pi^*_{C2-C3}$	0.51	0.51	< 0.5	0.51	< 0.5	< 0.5
		π^*_{C4-C5}	0.46854	$LP(1)_{N7} \rightarrow \pi^*_{C4-C5}$	44.53	44.73	45.22	44.72	44.40	43.63
		π^*_{C8-N10}	0.30326	$LP(1)_{N7} \rightarrow \pi^*_{C8-N10}$	60.07	60.39	59.25	60.42	58.29	57.08
		$\sigma^*_{C11-C12}$	0.02670	$LP(1)_{N7} \rightarrow \sigma^*_{C11-C12}$	4.89	4.97	5.00	5.00	4.73	4.52
		$\pi^*_{C11-C12}$	0.36802	$LP(1)_{N7} \rightarrow \pi^*_{C11-C12}$	8.34	7.99	8.90	6.88	11.06	13.12
		$\sigma^*_{C11-C16}$	0.02649	$LP(1)_{N7} \rightarrow \sigma^*_{C11-C16}$	4.89	4.89	4.85	5.26	4.53	4.34
$LP(1)_{S9}$	1.98211	σ^*_{C4-C5}	0.03264	$LP(1)_{S9} \rightarrow \sigma^*_{C4-C5}$	2.13	2.14	2.15	2.13	2.15	2.18
		σ^*_{C5-C6}	0.02103	$LP(1)_{S9} \rightarrow \sigma^*_{C5-C6}$	0.53	0.53	0.52	0.53	0.52	0.51
		σ^*_{N7-C8}	0.07155	$LP(1)_{S9} \rightarrow \sigma^*_{N7-C8}$	2.01	2.01	2.03	2.01	2.06	2.10
		σ^*_{C8-N10}	0.00937	$LP(1)_{S9} \rightarrow \sigma^*_{C8-N10}$	0.54	0.54	0.55	0.54	0.55	0.55
$LP(2)_{S9}$	1.77794	π^*_{C4-C5}	0.46854	$LP(2)_{S9} \rightarrow \pi^*_{C4-C5}$	19.95	19.99	23.29	19.94	23.23	23.28
		π^*_{C8-N10}	0.30326	$LP(2)_{S9} \rightarrow \pi^*_{C8-N10}$	30.82	30.77	31.19	30.81	31.46	31.79
$LP(1)_{N10}$	1.89453	σ^*_{N7-C8}	0.07155	$LP(1)_{N10} \rightarrow \sigma^*_{N7-C8}$	5.10	5.06	5.22	5.06	5.29	5.37
		σ^*_{N7-C11}	0.04266	$LP(1)_{N10} \rightarrow \sigma^*_{N7-C11}$	0.69	0.69	0.68	0.68	0.66	0.63
		σ^*_{C8-S9}	0.08416	$LP(1)_{N10} \rightarrow \sigma^*_{C8-S9}$	24.35	24.35	24.31	24.32	24.20	24.03

ED: electron density; NBO: natural bond orbital.

The FMOs of compounds **1**–**6** have been investigated at the M06-2x/6-311++G(d,p) level of theory. The corresponding energy levels of the FMOs for the studied compounds are given in Figure 3. Based on the investigation on the FMOs energy levels, we find that the corresponding electronic transfers happened between the HOMO and LUMO.

As can be seen in Table 4, the *para* functional group will further influence the HOMO and LUMO energy levels in the studied compounds (**1**–**6**). Electron-withdrawing substituents lead to a decrease in the energy levels of the frontier orbitals whereas electron-donating groups have the opposite effect. In this work, the energy levels increase in order from the most strongly electron-withdrawing group (–NO_2) to the most strongly electron-donating group (–CH_3). It is noted that 3-phenylbenzo[*d*]thiazole-2(3*H*)-imine has HOMO energy of −7.01 eV, and nitro-substituted derivatives (a nitro group being the strong electron-withdrawing group, and making the ring even more unreactive) have the HOMO energy of −7.42 eV. The nitro group in compound **6** is a very strong electrophile; that is, it has a strong ability to attract electrons. This ability can also be represented by the net charges of the nitro group. The higher the negative charge the nitro group possesses, the lower the electron attraction ability and therefore the more stable the nitro compound is. An electron-withdrawing group removes electrons and, therefore decreases the HOMO and LUMO energies. An electron-donating group usually acts through an occupied nonbonding orbital. This is energetically close to the HOMO. Thus, it has a stronger effect on the HOMO than on the LUMO (at least in organic molecules).

NBO analysis

NBO analysis has already proved to be an effective tool for the chemical interpretation of hyperconjugative interactions and electron density transfer from the filled lone-pair electron.[56] These changes in electron density are referred to as "delocalization" corrections to the zeroth-order natural Lewis structure to a stabilizing donor–acceptor interaction. In order to consider the different second-order perturbation energies (E_2) between the filled orbitals of one subsystem and the vacant orbitals of another subsystem, the M06-2x method has been used, and it predicts the delocalization or hyperconjugation.[57] In the NBO analysis, the charge transfer between the lone pairs of the proton acceptor and antibonding orbitals of the proton donor is the most important. For each donor NBO(*i*) and acceptor NBO(*j*), the stabilization energy (E_2) associated with the delocalization $i \rightarrow j$ is given by[58]

$$E_2 = \Delta E_{ij} = q_i \left(\frac{F^2_{(i,j)}}{\varepsilon_i - \varepsilon_j} \right) \quad (7)$$

where q_i is the *i*th donor orbital occupancy, ε_i and ε_j are diagonal elements (orbital energies), and $F_{(i,j)}$ is the off-diagonal NBO Fock matrix elements. The strong intramolecular hyperconjugative interactions of the σ and π electrons of C–C, C–H, N–H, and C–N to the antibonding C–C, C–H, N–H, and C–N bonds lead to stabilization of some part of the ring.[59] As can be seen in Table 5, the $\sigma \rightarrow \sigma^*$ interactions have minimum delocalization energy compared to the $\pi \rightarrow \pi^*$ interactions. Therefore, the σ bonds have higher electron density than the π bonds.

The strong intramolecular hyperconjugative interaction of the C4–C5 bond is formed by orbital overlap between the bonding orbital π_{C4-C5} to the corresponding antibonding orbital π^*_{C1-C6} with increasing electron density of 0.3581 leading to stabilization energy of 30.29 kcal/mol, which results in intramolecular charge transfer causing stabilization of the molecule. Similarly, $\pi \rightarrow \pi^*$ interactions take place between the bonding π_{C4-C5} and antibonding orbitals

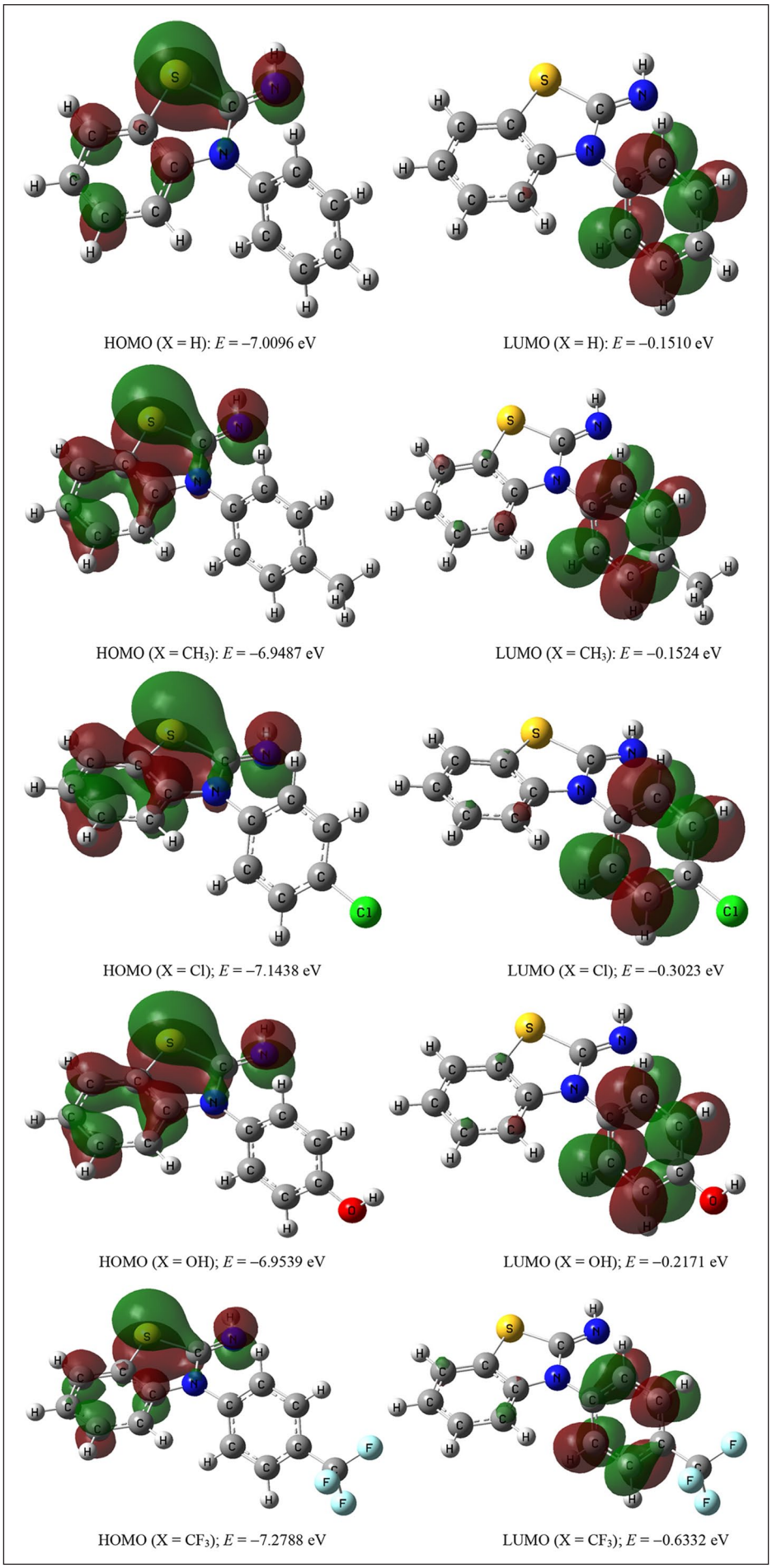

Figure 3. *(Continued)*

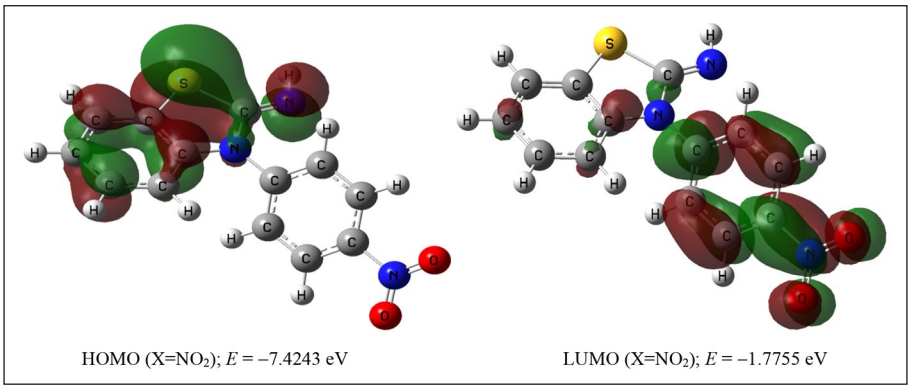

Figure 3. The shapes of the HOMO and LUMO orbitals of compounds **1**–**6** at the M06-2x/6-311++G(d,p) level.

$\pi^*_{C2–C3}$ as well as the bonding $\pi_{C8–N10}$ and antibonding orbitals $\pi^*_{C8–N10}$, with an increase in electron density of 0.3568 and 0.30326, respectively, such that the respective bonds are stabilized by 24.20 (strong) and 1.77 kcal/mol (weak), respectively.

The NBO analysis also describes the bonding in terms of the natural hybrid orbital which emphasizes that the lone pair of the nitrogen N7 has an exclusive *p*-character (>99.9%) and a low occupation number (1.67385 a.u.) in compounds **1**–**6**, leading to stronger stabilization interactions. Therefore, a very close to pure *p*-type lone-pair orbital participates in the electron donation to the $\pi^*_{C4–C5}$ antibonding orbital for the $LP(1)_{N7} \rightarrow \pi^*_{C4–C5}$ interaction, and $\pi^*_{C8–N10}$ antibonding orbital for the $LP(1)_{N7} \rightarrow \pi^*_{C8–N10}$ interaction in the considered compounds. The results are given in Table 5.

It is noted that the lone-pair $LP(1)N_{10}$ nitrogen atom occupies a higher energy orbital (1.89453 a.u.) with *p*-character of ~34.4%. Also, the other lone-pair $LP(1)_{S9}$ sulfur atom has a high occupation number (1.98211 a.u.) with *p*-character (~63%). The lone-pair electrons are readily available for interactions with the excited electrons of the acceptor antibonding orbital. The $LP(n) \rightarrow \pi^*$ interaction from nonbonding N_7, $LP(1)_{N7}$ donates an electron to the antibonding $\pi^*_{C8–N10}$ and $\pi^*_{C4–C5}$ orbitals with considerably higher stabilization energies of 60.07 and 44.53 kcal/mol, respectively. Similarly, intramolecular hyperconjugative interactions from the nonbonding S9 atom, $LP(2)_{S9}$ to $\pi^*_{C8–N10}$ and $\pi^*_{C4–C5}$ occur, leading to the stabilization energies of 30.82 and 19.95 kcal/mol, respectively. While the $LP(n) \rightarrow \sigma^*$ interaction takes place between the nonbonding N10 atom, $LP(1)_{N10}$ to the $\sigma^*_{C8–S9}$ antibonding orbital with the highest stabilization energy of 24.35 kcal/mol which results in intramolecular charge transfer causing stabilization of the molecular system.

NICS analysis

Aromaticity is a significant parameter related to cyclic arrays of mobile electrons and is a useful tool in organic chemistry.[60] Theoretical criteria of aromaticity allow information on the physico-chemical properties of aromatic rings, namely structural chemical reactivity and stability. Schleyer et al.[61] developed a simple and effective criterion for determining the aromaticity of different systems based on the diatropic current induced on placing the aromatic system in an external magnetic field. The NICS parameter was calculated as the negative shielding constant of a ghost atom (Bq) located at the ring center. Negative NICS values indicate a diatropic ring current in the presence of an applied magnetic field (aromatic molecule), while a low negative or positive NICS value indicates a paratropic ring current (non-aromatic or anti-aromatic molecule).[62,63] NICS values were taken at a location near the geometrical center of the ring.

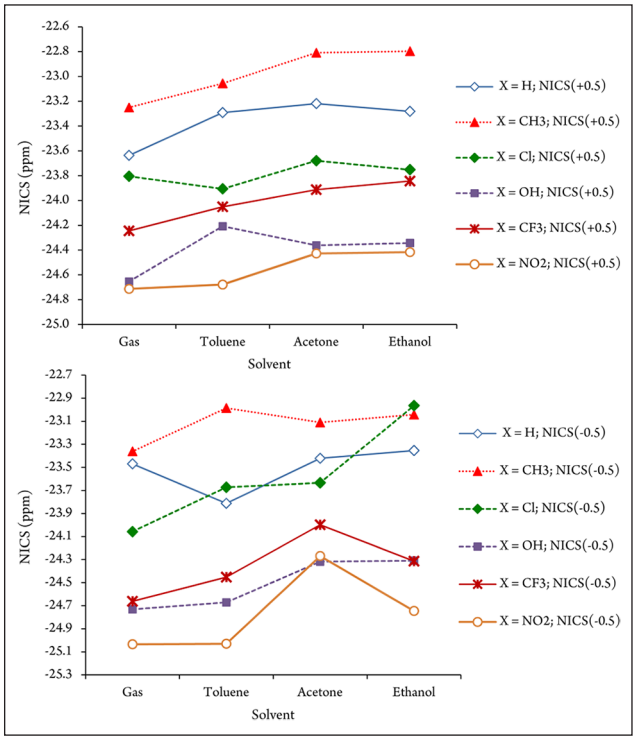

Figure 4. Overall aromaticity of the studied compounds estimated as a function of NICS versus the considered solvents. NICS values at maximum diatropic current are tabulated [*up*: NICS(+0.5); *down*: NICS(−0.5)].

In this study, for 3-phenylbenzo[*d*]thiazole-2(3*H*)-imines **1**–**6**, the sets of points (Bq ghost atoms) lying above and below, geometric center of rings were used at 2 Å. Their locations correspond with distances from −2 to 2 Å with 0.5 Å steps. The NICS(0) values are calculated at the center of the ring that is influenced by σ-bonds, while the NICS(+2) and NICS(−2) values determined at 2 Å above

and below the plane, respectively, were more affected by the π-electron system. The maximum total diatropic current is observed at 0.5 Å above/below the geometric center of molecule in compounds **1**–**6** (Figure 4).

Interestingly, the NICS values at the minimum point of the six-membered rings are more negative (i.e. indicating greater aromaticity) than those of the five-membered rings for all the considered compounds (see Table S2 of the Supplemental material). As can be seen from Table S2, the NICS values of compound **2** in the studied solvent and gas phases were calculated to be in ranges of −22.7965 to −23.2507 ppm, while the NICS values of compound **6** were slightly higher ranging from −24.4163 to −24.7124 ppm. For points located at the center of the six- and five-membered rings and points located at ±2 Å, the ring centers confirm that the aromaticity of compounds **1**–**6** changes with the varying dielectric constant of the media (see Table S2 in the Supplemental material).

Conclusion

In this work, the solvation and substituent effects of the electron-releasing/withdrawing derivatives (i.e. at the *para* position on the three-substituted molecular structure of the synthesized compounds) **1**–**6** [**1** (X=H), **2** (X=CH_3), **3** (X=Cl), **4** (X=OH), **5** (X=CF3), and **6** (X=NO_2)] were investigated using at the DFT/M06-2x/6-311++G(d,p) level of theory in selected solvents (toluene, acetone, and ethanol) and in the gas phase by employing the polarizable continuum method model. In addition, the Fukui function, dipole moment, and distribution of electric charges on the atoms of the considered compounds were also studied with the same method and basis set.

FMO analysis showed that compound **6** in the selected solvents and gas phase has very low HOMO-LUMO energy gaps and thus is kinetically less stable. Chemical reactivity indices (dipole moment, μ) predict the highest activity for compound **6** in different solvents as well as in the gas phase, whereas the lowest activity was decreased for compounds **4** and **1** in the gas phase and the studied solvents, respectively. The lowest HOMO-LUMO band gap is calculated for compound **6**, which results in it having interesting electronic properties. The obtained HOMO-LUMO energy gap corresponds to intramolecular hyperconjugative interactions $\pi \rightarrow \pi^*$. The results were confirmed by FMO analysis with energy gaps of 6.859, 6.796, 6.841, 6.737, 5.649, and 6.649 eV, respectively, being determined for molecules **1**–**6.** The calculated results show that molecules **1** and **6** have the highest and lowest stabilities, respectively, in the solvent and gas phases. NBO analysis showed intramolecular charge transfer causing stabilization of the molecule.

Acknowledgements

The authors would like to thank the referees for their valuable comments which helped to improve the manuscript.

Declaration of conflicting interests

The author(s) declared no potential conflicts of interest with respect to the research, authorship, and/or publication of this article.

Funding

The author(s) received no financial support for the research, authorship, and/or publication of this article.

ORCID iD

Abolfazl Shiroudi https://orcid.org/0000-0002-0765-6315

Supplemental material

Supplemental material for this article is available online.

References

1. Asif M. *Int J Bioorg Chem* 2017; 2: 146.
2. Marzi M, Shiroudi A, Pourshamsian K, et al. *J Sulfur Chem* 2019; 40: 166.
3. Saini MS, Kumar A, Dwivedi J, et al. *Int J Pharma Sci Res* 2013; 4: 66.
4. Chhabra M, Sinha S, Banerjee S, et al. *Bioorganic Med Chem Lett* 2016; 26: 213.
5. Jiang J, Li G, Zhang F, et al. *Adv Synth Catal* 2018; 360: 1622.
6. Haroun M, Tratrat C, Kositzi K, et al. *Curr Top Med Chem* 2018; 18: 75.
7. Rabbani MG, Islamoglu T and El-Kaderi HM. *J Mater Chem A* 2017; 5: 258.
8. Gill RK, Rawal RK and Bariwal J. *Arch Pharm* 2015; 348: 155.
9. Diao P-C, Lin W-Y, Jian X-E, et al. *Eur J Med Chem* 2019; 179: 196.
10. Abdelgawad MA, Bakr RB and Omar HA. *Bioorg Chem* 2017; 74: 82.
11. Ali R and Siddiqui N. *J Chem* 2013; 345198.
12. Das D, Sikdar P and Bairagi M. *Eur J Med Chem* 2016; 109: 89.
13. Aitken L, Benek O, McKelvie BE, et al. *Molecules* 2019; 24: 2757.
14. Shuai L and Luterbacher J. *ChemSusChem* 2016; 9: 133.
15. Noviandri I, Brown KN, Fleming DS, et al. *J Phys Chem B* 1999; 103: 6713.
16. Pirbasti FG and Mahmoodi NO. *J Chin Chem Soc Taip* 2016; 64: 80.
17. Kurt M, Sertbakan TR and Ozduran M. *Spectrochim Acta A Mol Biomol Spectrosc* 2008; 70: 664.
18. Onsager L. *J Am Chem Soc* 1936; 58: 1486.
19. Rivail L and Rinaldi D. *Theor Chim Acta* 1973; 32: 57.
20. Hall RJ, Davidson MM, Burton NA, et al. *J Phys Chem* 1995; 99: 921.
21. Zhao Y and Truhlar DG. *Theor Chem Acc* 2008; 120: 215.
22. Dunning TH. *J Chem Phys* 1989; 90: 1007.
23. Sastre S, Casasnovas R, Muñoz F, et al. *Theor Chem Acc* 2013; 132: 1310.
24. Junqueira GMA and Dos Santos HF. *J Mol Model* 2014; 20: 2152.
25. Cysewski P. *J Mol Struct (Theochem)* 2005; 714: 29.
26. Nigam S, Majumder C and Kulshreshtha SK. *J Chem Sci* 2006; 118: 575.
27. Schleyer PVR, Manoharan M, Wang Z-X, et al. *Org Lett* 2001; 3: 2465.
28. Schleyer PVR, Jiao H, Goldfuss B, et al. *Angew Chem Int Ed Engl* 1995; 34: 337.
29. Schleyer PVR, Maerker C, Dransfeld A, et al. *J Am Chem Soc* 1996; 118: 6317.
30. Reed AE, Weinstock RB and Weinhold F. *J Chem Phys* 1985; 83: 735.

31. Badenhoop JK and Weinhold F. *Int J Quantum Chem* 1999; 72: 269.
32. Nori-Shargh D, Shiroudi A, Oliaey AR, et al. *J Mol Struct (Theochem)* 2007; 824: 1.
33. Frisch MJ, Trucks GW, Schlegel HB, et al. *Gaussian 09*. Wallingford, CT: Gaussian Inc, 2009.
34. Dennington R, Keith T and Millam J. *Gauss View 5.0*. Shawnee, KS: Semichem Inc, 2009.
35. Baboul AG, Curtiss LA and Redfern PC. *J Chem Phys* 1999; 110: 7650.
36. Halls MD, Velkovski J and Schlegel HB. *Theor Chem Acc* 2001; 105: 413.
37. Senosiain JP, Klippenstein SJ and Miller JA. *J Phys Chem A* 2005; 109: 6045.
38. Greenwald EE, North SW, Georgievskii Y, et al. *J Phys Chem A* 2005; 109: 6031.
39. Zhao Y and Truhlar DG. *Acc Chem Res* 2008; 41: 157.
40. Zahedi E, Shaabani S and Shiroudi A. *J Phys Chem A* 2017; 121: 8504.
41. Glendening ED, Badenhoop JK, Reed AE, et al. *NBO 5.0*. Madison, WI: Theoretical Chemistry Institute, University of Wisconsin, 2001.
42. Shiroudi A, Safaei A, Kazeminejad Z, et al. *J Mol Model* 2020; 26: 57.
43. Demir S, Tinmaz F, Dege N, et al. *J Mol Struct* 2016; 1108: 637.
44. Mottishaw JD, Erck AR, Kramer JH, et al. *J Chem Educ* 2015; 92: 1846.
45. Mulliken R. *J Chem Phys* 1955; 23, 1841.
46. Mulliken R. *J Chem Phys* 1962; 36, 3428.
47. Rigby J and Izgorodina EI. *Phys Chem Chem Phys* 2013; 15, 1632.
48. Fukui K, Yonezawa T and Shingu H. *J Chem Phys* 1952; 20: 722.
49. Padmaja L, Ravikumar C, Sajan D, et al. *J Raman Spectrosc* 2009; 40: 419.
50. Aihara J. *J Phys Chem A* 1999; 103: 7487.
51. Manolopoulos ED, May JC and Down SE. *Chem Phys Lett* 1991; 181: 105.
52. Ruiz-Morales Y. *J Phys Chem A* 2002; 106: 11283.
53. Parr RG, Szentpaly L and Liu S. *J Am Chem Soc* 1999; 121: 1922.
54. Parr RG and Pearson RG. *J Am Chem Soc* 1983; 105: 7512.
55. Parr RG, Donnelly RA, Levy M, et al. *J Chem Phys* 1978; 68: 3801.
56. Yang Y, Zhang W and Gao X. *Int J Quantum Chem* 2006; 106: 1199.
57. Carpenter JE and Weinhold F. *J Mol Struct (Theochem)* 1988; 169: 41.
58. Oliaey AR, Shiroudi A, Zahedi E, et al. *React Kinet Mech Cat* 2018; 124: 27.
59. Durga Devi D, Manivarman S and Subashchandrabose S. *Karbala Int J Mod Sci* 2017; 3: 18.
60. Gangadharana RP and Krishnanb SS. *Acta Phys Pol A* 2014; 125: 18.
61. Schleyer PVR and Jiao H. *Pure Appl Chem* 1996; 68: 209.
62. Krygowski TM, Cyranski M, Ciesielski A, et al. *J Chem Inf Comput Sci* 1996; 36: 1135.
63. Badoglu S and Yurdakul S. *Struct Chem* 2010; 21: 1103.